

## Microstructure and Phase Behavior of Concentrated Silica Particle Suspensions

Jae-Hyun So, Won-Kyoung Oh and Seung-Man Yang<sup>†</sup>

Department of Chemical and Biomolecular Engineering, 373-1, Guseong-dong, Yuseong-gu, Daejeon 305-701, Republic of Korea

(Received 28 January 2004 • accepted 22 June 2004)

**Abstract**—Dispersion stability and microstructural transition of colloidal silica suspensions were examined by rheological measurements under either steady simple shear or oscillatory flow. Monodisperse silica particles were prepared by the so-called modified Stöber method and were stabilized by either steric or electrostatic repulsive force. Depending upon the methods of stabilization, the suspension showed hard-sphere or soft-sphere response. In particular, silica suspensions exhibited hard-sphere response when the silica spheres coated with 3-(trimethoxysilyl)propyl methacrylate (MPTS;  $(\text{CH}_3\text{O})_3\text{Si}(\text{CH}_2)_3\text{OCOC}(\text{CH}_3)=\text{CH}_2$ ) were dispersed in a refractive-index matching solvent, tetrahydrofurfuryl alcohol. On the other hand, silica particles in aqueous media behaved like soft spheres with long-range electrostatic repulsive interactions when they were coated with steric layer of aminosilane coupling agent, N-[3-(trimethoxysilyl)propyl]ethylenediamine  $((\text{CH}_3\text{O})_3\text{Si}(\text{CH}_2)_3\text{NHCH}_2\text{CH}_2\text{NH}_2)$ . In this case, the electrostatic repulsion or equivalently the softness of the silica spheres was controlled by the ionic strength using a symmetric salt KCl. Both the hard-sphere and soft-sphere suspensions showed stable shear-thinning behavior without experiencing shear-induced flocculation. Moreover, the oscillatory shear rheology showed that the electrostatically stabilized soft-sphere suspensions underwent a microstructural transition from liquid-like to solid-like structure when either the particle loading increased or the ionic strength was reduced.

Key words: Dispersion Stability, Silica Suspension, Silane Coupling Agent, Microstructure, Phase Transition, Hard Spheres, Soft Spheres, Rheological Behavior

### INTRODUCTION

The flow behavior and microstructure of colloidal particle dispersions have been studied intensively because of their practical significance in paints, polymers, ceramics, composite materials, coating processes, as well as the electronic industry [Lewis, 2000]. In particular, metal oxide suspensions have attracted considerable attention in dispersion stabilization and the electronic materials [Tadros, 1996; So et al., 2001a, b].

Usually, particle dispersion shows non-Newtonian behavior even though the medium is a Newtonian liquid. Deviation from the Newtonian flow behavior becomes pronounced at high particle volume fractions and under strong flow field due to the predominant interparticle interactions. As the imposed flow becomes strong, semi-dilute and concentrated suspensions often exhibit shear thinning and/or shear thickening, following a gradual decrease or increase in the shear viscosity. Practically, continuous or discontinuous shear thickening causes severe damage on the particulate process and eventually deteriorates productivity [Barnes, 1989a, b]. Therefore, it is necessary to investigate the microstructural changes of particulate suspensions, and thereby to control the rheological properties under flow field. The flow characteristics of particulate suspensions can be controlled by the particle shape, size distribution, interparticle forces, and the volume fraction of the dispersed phase.

In general, monodisperse hard sphere suspension begins to order into a macrocrystalline structure of face centered cubic (FCC) or hexagonally close packing (HCP), when the particle volume fraction ( $\phi$ ) exceeds 0.5 under equilibrium condition with no imposed

flow. Further, when  $0.5 < \phi < 0.55$ , the random disordered phase and the colloidal crystalline phase coexist [Russel et al., 1989; Gast and Russel, 1998; Larson, 1999]. However, charge stabilized suspensions form macrocrystalline structure at much lower volume fractions compared with hard sphere suspensions. This is due to stronger long-range repulsive interparticle interactions of electrostatically stabilized suspension [Russel et al., 1989; Kose et al., 1973; Kose and Hachisu, 1976; Chen et al., 1994; Chow and Zukoski, 1995a]. Therefore, charge stabilized polymer latices such as polystyrene or polymethylmethacrylate show 'soft' sphere behavior; the rheological responses of these latex suspensions have been studied extensively [Chen et al., 1994; Chow and Zukoski, 1995a, b; Laun et al., 1992]. Recently, some works have been reported about the rheological behavior and interparticle interactions of charge stabilized metal oxide particle suspensions such as silica and alumina [Fagan and Zukoski, 1997; Franks et al., 2000]. However, the microstructural transitions and rheological behavior in terms of the interparticle interactions have not been clearly explained and it is still challenging to study comprehensively by taking into account both the interparticle forces and the types and strength of flow.

In the present study, the rheological behavior of silica particle suspensions was examined by varying the strength of the interparticle forces. Monodisperse spherical silica particles have been synthesized successfully through sol-gel method [Stöber et al., 1968; Bogush et al., 1988; Philipse and Vrij, 1989]. In our group, the stabilization effects and microstructural changes for hard sphere silica suspensions have been considered by using various silane coupling agents, vinyltriethoxy silane (VTES),  $\gamma$ -methacryloxypropyl triethoxy silane (MPTES) and 3-(trimethoxysilyl)propyl methacrylate (MPTS) [Lee and Yang, 1998; Lee et al., 1999; So et al., 2001c, d]. The synthesized monodisperse silica particles can be stabilized with a silane

<sup>†</sup>To whom correspondence should be addressed.

E-mail: smyang@kaist.ac.kr

coupling agent and used for the preparation of sterically stabilized suspension in either organic or aqueous medium, which show hard sphere or soft sphere characteristics. Particularly, silica particles in aqueous medium possess substantial surface charges. Consequently, the silica particles are stabilized predominantly by electrostatic repulsion when the thickness of steric barrier is much smaller than the range of the electrostatic repulsion. Meanwhile, the electrostatic repulsive forces can be controlled by varying the ionic strength (or salt concentration) and pH. In the subsequent sections, the dispersion stability was examined by measuring rheological responses of the stabilized silica suspensions under steady shear flow. In addition, the microstructural transition of aqueous silica suspensions from liquid-like to solid-like structure was confirmed by monitoring the storage modulus ( $G'$ ) under oscillatory shear flow for various particle volume fractions and salt concentrations. Finally, a phase diagram in terms of the particle volume fraction and ionic strength was constructed by the rheological responses under oscillatory flow for electrostatically stabilized silica particle suspensions.

## EXPERIMENTAL

Monodisperse silica particles were synthesized through the so-called modified Stöber method in ethanol (Oriental Chem.) medium. Tetraethylorthosilicate (TEOS;  $\text{Si}(\text{OC}_2\text{H}_5)_4$ , Aldrich) and deionized water were used as reactants for preparation of the spherical silica particles with the aid of ammonium hydroxide (Aldrich) as a reaction and morphological catalyst. Ethanol was purified twice by distillation and all other chemicals were used as received. The particle size was controlled by varying the concentrations of water and ammonia. In order to prepare concentrated monodisperse silica suspensions, hydrolysis and condensation reactions were conducted by step-wise dosage of silicon alkoxide precursor, TEOS with the time interval of 12 hrs as suggested by Bogush et al. [1988]. In this way, monodisperse model silica particles with different size were obtained. Detailed compositions of the reactants, particle sizes and BET surface areas of the silica particles prepared by a single step and three-step synthetic processes were summarized in Table 1. Hereafter, large and small model silica particles are designated as S51 and S13, respectively.

For the preparation of hard-sphere suspensions, 3-(trimethoxysilyl) propyl methacrylate (MPTS;  $(\text{CH}_3\text{O})_3\text{Si}(\text{CH}_2)_3\text{OCOC}(\text{CH}_3)=\text{CH}_2$ , Aldrich) were coated on the purified silica particles by chemical adsorption after step-wise particle synthesis. The prepared silica particles were purified by washing 6-7 times with distilled ethanol and ultracentrifugation. To ensure hard-sphere suspensions by screening the van der Waals attraction, tetrahydrofurfuryl alcohol (THFA, Aldrich) was used as a refractive-index ( $n_D=1.45$ ) matching sol-

vent. Through the surface modification of silica particles, any residual interparticle interaction could be removed effectively and the suspension showed 'hard sphere' behavior. The detailed procedure of the surface modification and adsorption behavior of MPTS onto silica particles were described in the literature [Lee et al., 1999; So et al., 2001c, d]. Hereafter, the MPTS coated hard-sphere suspensions are designated as HS13M or HS51M according to their particle sizes.

Meanwhile, electrostatically stabilized silica suspensions with long-range repulsive interactions were prepared in aqueous medium. In this case, the silica surface was modified with relatively short aminosilane coupling agent, N-[3-(Trimethoxysilyl)propyl]ethylenediamine ( $(\text{CH}_3\text{O})_3\text{Si}(\text{CH}_2)_3\text{NHCH}_2\text{CH}_2\text{NH}_2$ , Aldrich). Synthesized stock silica particles were washed with deionized water and ultracentrifuged 7 or 8 times in order to remove residual reactants. Then, the cleaned silica particles were coated with amino silane coupling agent, N-[3-(Trimethoxysilyl)propyl]ethylenediamine in deionized water. After the surface modification with aminosilane coupling agent, silica particles were separated from the mixture by ultracentrifugation and re-dispersed in distilled water. The ionic strength was controlled by changing KCl concentration from  $10^{-3}$  to  $10^{-1}$  M. In order to increase the particle loading, the silica suspension was dialyzed against a dilute aqueous polyethyleneglycol (PEG, M.W.=20,000; Junsei) solution. During dialysis, the salt concentration was also adjusted by using a dialysis membrane with molecular weight cut-off of 6,000-8,000. The KCl dialysis solutions with dissolved PEG were replaced with a fresh one several times in 48 hr. The resulting particle suspensions were aged for at least three weeks and henceforth designated as S13S and S51S according to the particle size. The concentrated suspensions at low salt concentrations were slightly iridescent or exhibited a slightly bluish hue because of Bragg diffraction.

In order to determine the particle volume fraction, the density of suspended silica particle was estimated from the intrinsic viscosity of monodisperse spherical suspension at extreme dilutions. By measuring the viscosity for extremely dilute suspensions using an Ubbelohde capillary viscometer, we determined the density of prepared silica particles as  $1.62 \times 10^{-3} \text{ kg/m}^3$ ,  $1.70 \times 10^{-3} \text{ kg/m}^3$  for S13 and S51, respectively [So et al., 2001c, d]. The weight fraction of each suspension was converted to the volume fraction by using the pre-determined density value.

For charged silica particles, the  $\zeta$ -potential of silica suspension was measured by the electrophoretic light scattering (Brookhaven); the result is shown in Table 2. The rheological behavior was monitored by a fluid rheometer (ARES) under either steady or oscillatory shear flow in Couette geometry. A series of steady shear viscosity measurements were performed after the samples were pre-

**Table 1. Compositions of the reactants in synthesis of model silica particles, BET surface area, and adsorbed amount of coupling agent**

	Reactant composition	Mean radius [nm]	BET surface area [m <sup>2</sup> /g]	Number of adsorbed coupling agent [/(nm <sup>2</sup> SiO <sub>2</sub> )]	
				Amino silane	MPTS
S13	[TEOS]=0.57+0.57+0.57+0.57 M, [NH <sub>3</sub> ]=0.35 M, [H <sub>2</sub> O]=0.85 M	108.52±5.55	13.04	11.6 (S13S)	82.2 (HS13M)
S51	[TEOS]=0.57+0.57 M, [NH <sub>3</sub> ]=0.71 M, [H <sub>2</sub> O]=5.0 M	272.78±1.97	5.97	22.7 (S51S)	116.8 (HS51M)

**Table 2.  $\zeta$ -Potential of the stabilized model silica particle suspensions**

	Bare aqueous suspensions	Modified with amino silane in aqueous medium			Modified with MPTS in THFFA
Salt concentration	$10^{-3}$ M	$10^{-3}$ M	$10^{-2}$ M	$10^{-1}$ M	-
S13S/HS13M	$-52.7 \pm 2.5$ mV	$-48.6 \pm 2.8$ mV	$-39.4 \pm 2.1$ mV	$-12.8 \pm 4.5$ mV	$-0.9 \pm 0.4$ mV
pH	pH=9.13	pH=8.86	pH=8.48	pH=8.45	-
S51S/HS51M	$-63.3 \pm 2.9$ mV	$-47.2 \pm 3.8$ mV	-	-	$-0.8 \pm 0.5$ mV
pH	pH=8.88	pH=8.10	-	-	-

sheared at a constant shear rate of  $0.025 \text{ s}^{-1}$  for 60 s. Frequency sweep measurements in oscillatory shear flow were performed in the range of linear viscoelasticity predetermined by strain sweep test. All rheological measurements were conducted at a fixed temperature of  $25^\circ\text{C}$ .

## RESULTS AND DISCUSSIONS

### 1. Characterization of the Model Silica Suspensions

The synthesized monodisperse silica particles were spherical and the average particle radii of S13 and S51 were  $108.52 \pm 5.52 \text{ nm}$  and  $272.78 \pm 1.97 \text{ nm}$ , as shown in Table 1. It can be noted that high ammonia content produced large particles with uniform size distribution.

To confirm the adsorption of various silane coupling agents onto the silica particles, adsorption behavior was characterized in our previous report [So et al., 2001d]. The adsorption isotherm of MPTS onto silica particles was determined by monitoring of free MPTS concentrations using UV-visible spectroscopy. Clear supernatant solutions containing free silane coupling agent were separated by ultra-centrifugation after the MPTS modification. Those results were fitted to Langmuir-type adsorption equation and saturated adsorption amounts were shown in Table 1. In addition, the adsorption behavior of aminosilane coupling agent was also characterized. The adsorbed amount of aminosilane coupling agent was directly measured by monitoring the nitrogen element level of the model silica particles. After surface modification with aminosilane coupling agent, silica particles were separated from the mixture of aminosilane coupling agent and aqueous stock silica suspension by ultracentrifugation. The adsorbed amounts of nitrogen were determined by element analysis and normalized with the results for bare silica particles. These adsorbed amounts were fitted to Langmuir-type adsorption equation and the saturated adsorption amounts per BET surface area were also shown in Table 1. From those saturated adsorption amounts, the effect of ammonium hydroxide, which is morphological catalyst in synthesizing step, was considerable in the adsorption process of silane coupling agent. Although the normalized adsorbed amounts of coupling agent for different sized particles are usually fitted on the same curve, the chemically adsorbed amounts of silane coupling agent deviate as given in Table 1 for MPTS and amino silane coupling agent. Those deviations could be explained by the differences in surface hydroxyl group densities for each model silica particles, which could be originating in different ammonium hydroxide dosage.

The  $\zeta$ -potentials of the bare and surface modified silica particles are listed in Table 2. The  $\zeta$ -potentials of silica spheres were given for various salt concentrations in aqueous medium or organic sol-

vent. As noted, for both bare and salt controlled suspensions, the pH was around 8-9. Thus, for aqueous suspensions, pH was maintained far above the isoelectric point although it slightly decreased

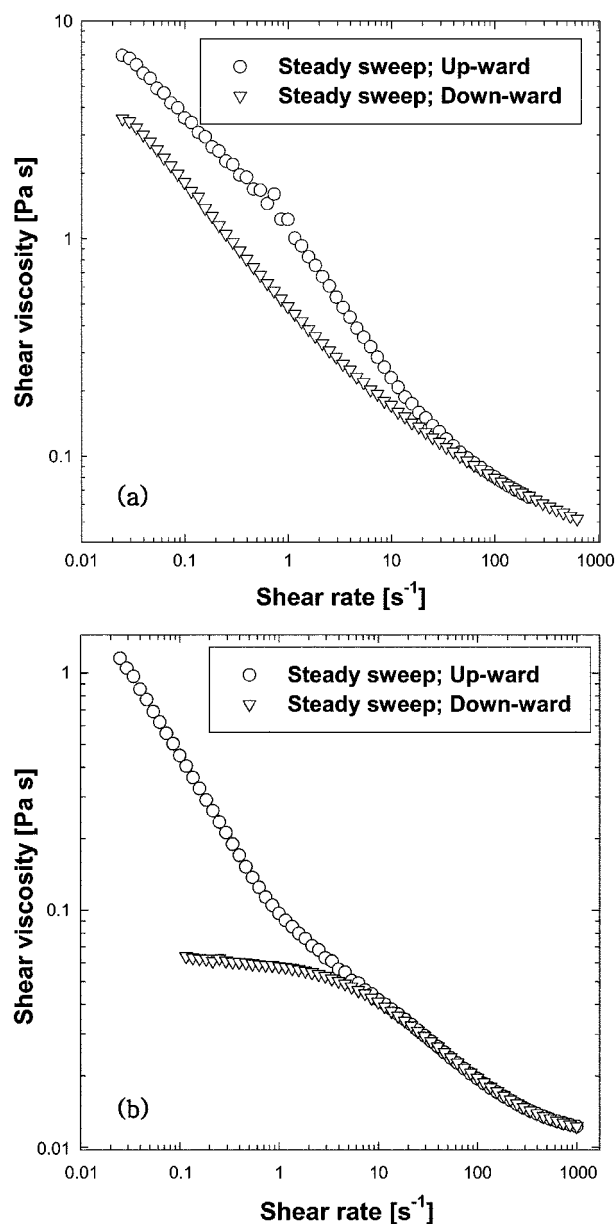


**Fig. 1.** Shear viscosity as a function of the steady shear rate during the upward and downward shear-rate sweep tests for (a) S51 bare silica suspension of  $\phi=0.48$  with  $[\text{KCl}]=10^{-3} \text{ M}$ , (b) S13 bare silica suspension of  $\phi=0.40$  with  $[\text{KCl}]=10^{-3} \text{ M}$ .

by the surface modification and salt addition. For the MPTS coated silica particles in organic solvent, the  $\zeta$ -potential was vanishingly small. Meanwhile, silica particles that were coated with aminosilane and dispersed in aqueous medium showed slightly weaker  $\zeta$ -potential than bare silica particles. However, the coated silica particles still possessed highly negative  $\zeta$ -potential and were effectively stabilized by surface charge. Moreover, the surface charge density was decreased with an increase in the ionic strength of KCl. This clearly indicates that the presence of salts decreases both the range and the magnitude of electrostatic repulsion by reducing the Debye shielding length and the  $\zeta$ -potential [Oh et al., 1999; So et al., 2001d].

## 2. Steady-state Rheological Behavior and Phase Stability of Silica Suspensions

Generally, deviations from Newtonian behavior are induced by the combined contributions from the hydrodynamic and non-hydro-

dynamic interparticle interactions and random Brownian motions under shear field. Thus, the rheological behavior of the semi-dilute or concentrated suspensions may be very complicated compared to other homogeneous fluids. Therefore, studies on the flow behavior and stability of concentrated suspensions are practically important [Lewis, 2000; Perez et al., 2002; Quemada and Betli, 2002; Stavov et al., 2002]. In Figs. 1(a) and (b), shear viscosities of bare silica suspensions of S51 and S13 were plotted for upward and downward shear-rate sweep tests. The particle volume fraction ( $\phi$ ) was fixed at either 0.48 or 0.40 and the salt (KCl) concentration was adjusted to  $10^{-3}$  M. It is noteworthy that stable colloidal dispersions showed no hysteresis in the shear viscosity versus shear rate during upward and downward shear-rate sweep measurements. As noted from Fig. 1, however, concentrated bare silica suspensions showed appreciable hysteresis at low shear rates. This was clearly because the bare silica suspensions were weakly flocculated and those floc-

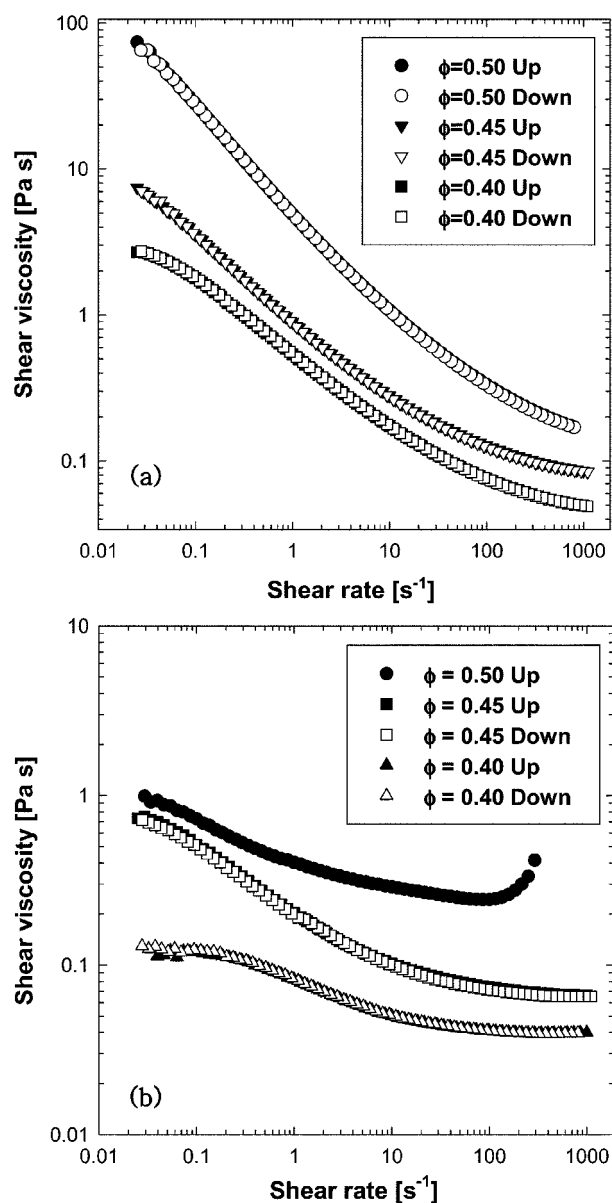


Fig. 2. Shear viscosity as a function of the steady shear rate during the upward and downward shear-rate sweep tests for (a) HS13M, (b) HS51M.

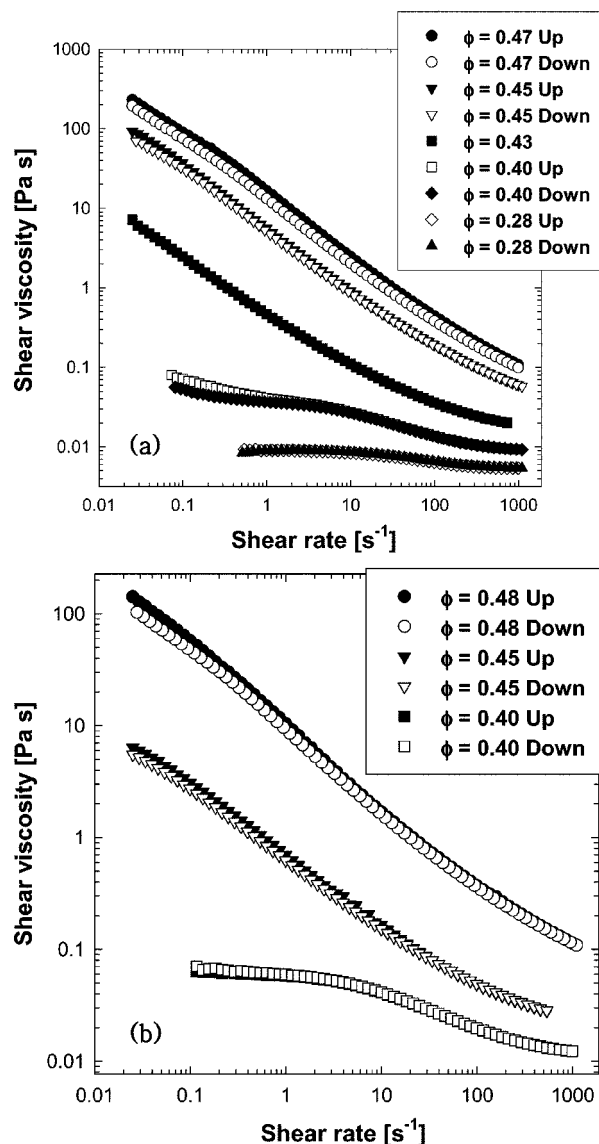


Fig. 3. Shear viscosity as a function of the steady shear rate during the upward and downward shear-rate sweep tests for (a) S13S with [KCl]= $10^{-3}$  M, (b) S13S with [KCl]= $10^{-2}$  M.

culated structures were destroyed under shear field. Therefore, additional steric barriers were needed to give sufficient stability by adsorption of silane coupling agent onto the silica particle surface as described previously.

In Figs. 2(a) and (b), steady shear viscosity of hard sphere suspensions (HS13M and HS51M) stabilized with MPTS are shown at various volume fractions. As noted, there was no viscosity hysteresis during upward and downward shear rate sweeps, which was indicative of the fact that those model suspensions were well stabilized in the refractive-index matching organic medium. In case of HS51M, shear thickening was observed at  $\phi=0.50$ , which was due to the considerable interparticle interactions at high shear rates [Chow and Zukoski, 1995b; Stavov et al., 2002].

In Figs. 3(a) and (b), shear viscosity of S13S suspension stabilized electrosterically was plotted as a function of the shear rate for various particle volume fractions with  $[KCl]=10^{-3}$  M and  $10^{-2}$  M, respectively. Similar to the previous observations in Figs. 2(a) and (b), typical shear thinning behavior was also observed. Moreover, up to the highest volume fractions of this study, no hysteresis was observed, indicating that those model suspensions were also sufficiently stabilized electrosterically. It can be noted from comparison of Fig. 3(a) and (b) that as the salt concentration increased, the shear viscosity was reduced. This can be explained by the fact that the screening effect of KCl and consequent compression of the electrical double layer led to the decrease of the effective volume fraction. Indeed, as noted from Table 2, the magnitude of  $\zeta$ -potential was decreased with the increase in the ionic strength. Moreover, the decrease in the shear viscosity became pronounced at low shear rates where the interparticle force was dominant. It can be also seen that when the particle volume fraction was lower than 0.40, the zero-shear-rate viscosity was measurable. This is because at low particle volume fractions the suspension had nearly random and isotropic structure and behaved like Newtonian fluids. Therefore, the viscosity at low shear rates showed a Newtonian plateau. Meanwhile, when the particle loading exceeded 0.40, the suspensions did not exhibit the zero-shear-rate viscosity, and instead the viscosity shear thinned continuously. This is due to the fact that some microstructure was formed at high concentrations at equilibrium, and this microstructure was deformed under the imposed shear flow [Foss and Brady, 2000; Brady, 2001].

In order to consider the effects of  $[KCl]$  on the flow behavior of the silica suspensions, the relative shear viscosity was plotted in Figs. 4(a) and (b). Here, steady rheological behavior of small and large model particle suspensions was shown for various salt concentrations and two different volume fractions ( $\phi=0.45$  and 0.40). Also included for comparison was the relative viscosity of hard sphere suspensions (HS13M and HS51M), which had the same particle size. It can be readily noted that as the salt concentration increased, the relative viscosity decreased and approached the viscosity of the hard sphere suspension. This clearly implies that the long-range repulsive force diminished with the ionic strength and the charged silica particles at high salt concentrations behaved like hard spheres. As mentioned earlier, the increase in salt concentration enhances the screening effect and compresses the electric double layer, which reduces the depletion volume and consequently decreases the effective particle volume fraction. In particular, the change in shear viscosity as a function of the salt concentration was pronounced at low

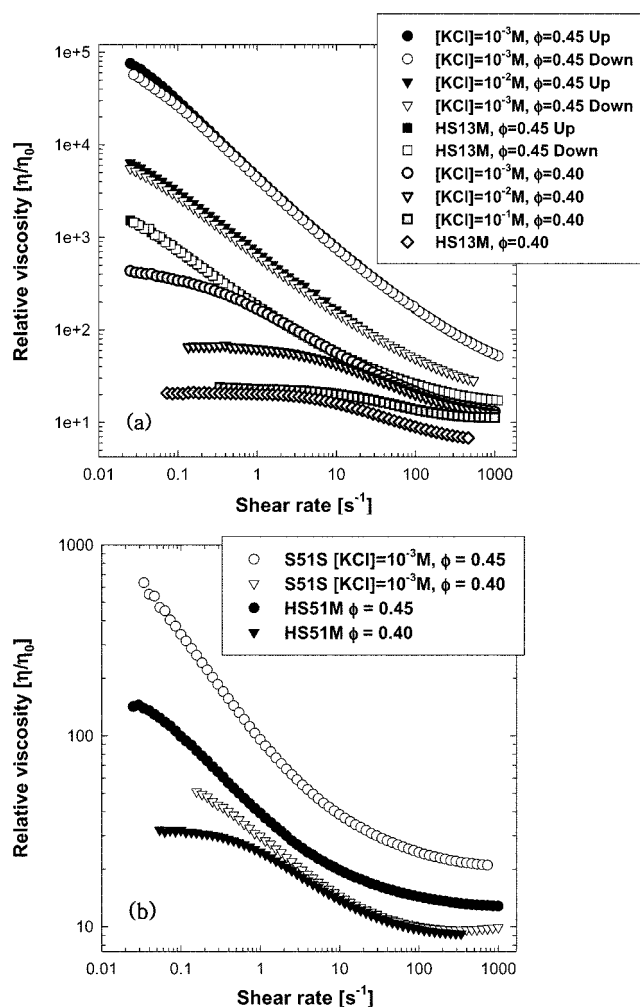


Fig. 4. Relative viscosity as a function of the shear rate for (a) S13S and HS13M at  $\phi=0.45$ , 0.40, (b) S51S and HS51M at  $\phi=0.45$ , 0.40.

shear rates in which the interparticle forces were dominant relative to hydrodynamic forces imposed by the shear flow. As the shear rate increased, the hydrodynamic contribution became dominant and the shear viscosities of charge-stabilized suspensions approached the viscosity of the hard sphere suspension with no interparticle interaction. This is independent of the salt concentration but dependent on the apparent particle volume fraction.

### 3. Microstructure Transitions of Stabilized Silica Particle Suspensions

Concentrated colloidal suspensions commonly display viscoelastic behavior, which is usually characterized by oscillatory measurement. Generally, microstructure of colloidal suspensions is classified by purely elastic (solid-like), purely viscous (liquid-like) and intermediate state [Russel et al., 1989; Larson, 1999; Lewis, 2000; Tadros, 1996]. In order to examine the microstructure of model particle suspension, storage ( $G'$ ) and loss ( $G''$ ) moduli were measured as a function of the sweep frequency at linear viscoelastic region. Particularly, we were interested in the storage modulus ( $G'$ ) versus the particle volume fractions and the salt concentrations to monitor the microstructural changes of model particle suspensions.

First, we considered the microstructure of S51S suspension at

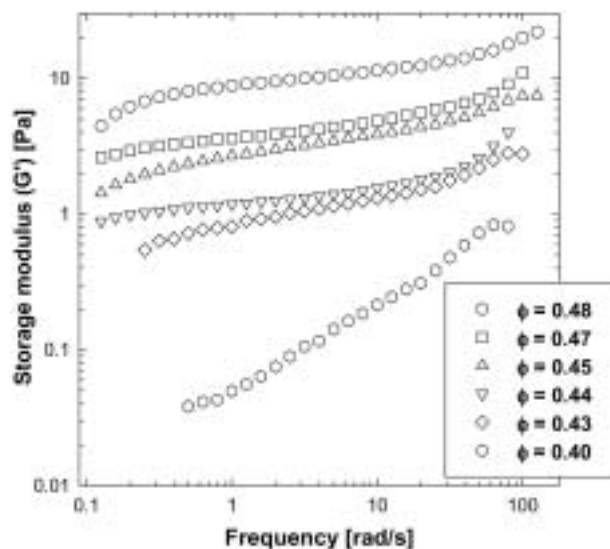


Fig. 5. Storage modulus ( $G'$ ) as a function of the frequency for charge stabilized S51S silica suspensions with  $[KCl]=10^{-3}$  M.

fixed salt concentration of  $10^{-3}$  M by measuring the storage modulus, which was reproduced in Fig. 5. As noted, a drastic change in storage modulus ( $G'$ ) was observed in dynamic measurements. The storage modulus was highly dependent on the frequency at low volume fractions, but became nearly independent of the frequency at high volume fractions. This is clearly indicative of the fact that those suspensions at low volume fractions exhibited typical liquid-like behavior and the microstructure changed from liquid-like structure to solid-like structure as the volume fraction increased.

In Figs. 6(a) and (b), the effects of particle volume fraction on the storage modulus were given as a function of the frequency for  $[KCl]=10^{-3}$  and  $10^{-2}$  M, respectively. At a fixed salt concentration, the storage modulus increased drastically as the volume fraction increased slightly from 0.40 to 0.47 or 0.48. Moreover, the storage modulus became nearly independent of the frequency with increase in the particle volume fractions. Also noted is that the storage modulus at  $[KCl]=10^{-3}$  M was larger than that at  $[KCl]=10^{-2}$  M. Indeed, at high salt concentrations, the charge stabilized suspensions displayed liquid-like behavior at the volume fraction of  $\phi=0.45$ . However, at a very low salt concentration  $[KCl]=10^{-3}$  M, the storage modulus ( $G'$ ) of the S13S suspension with the volume fraction of  $\phi=0.45$  showed solid-like behavior, i.e., very weak dependence on the frequency. Thus, at lower salt concentrations, the charge stabilized suspensions exhibited solid-like structure at relatively lower particle volume fractions.

In addition, the storage modulus ( $G'$ ) of S13S suspension was measured at  $\phi=0.45$  and 0.40 for various salt concentrations and the results were shown in Fig. 7(a). Also included in Fig. 7(b) was the storage modulus ( $G'$ ) of HS13M suspension, which behaved like 'hard-sphere' suspension as previously described. It is noteworthy at this point that the particle size of S13S was one half of S51S shown in Fig. 5. At high ionic strengths and low volume fractions, S13S suspension showed purely viscous behavior (liquid-like structure). However, as the salt concentration decreased and the particle volume increased, the S13S suspension experienced a

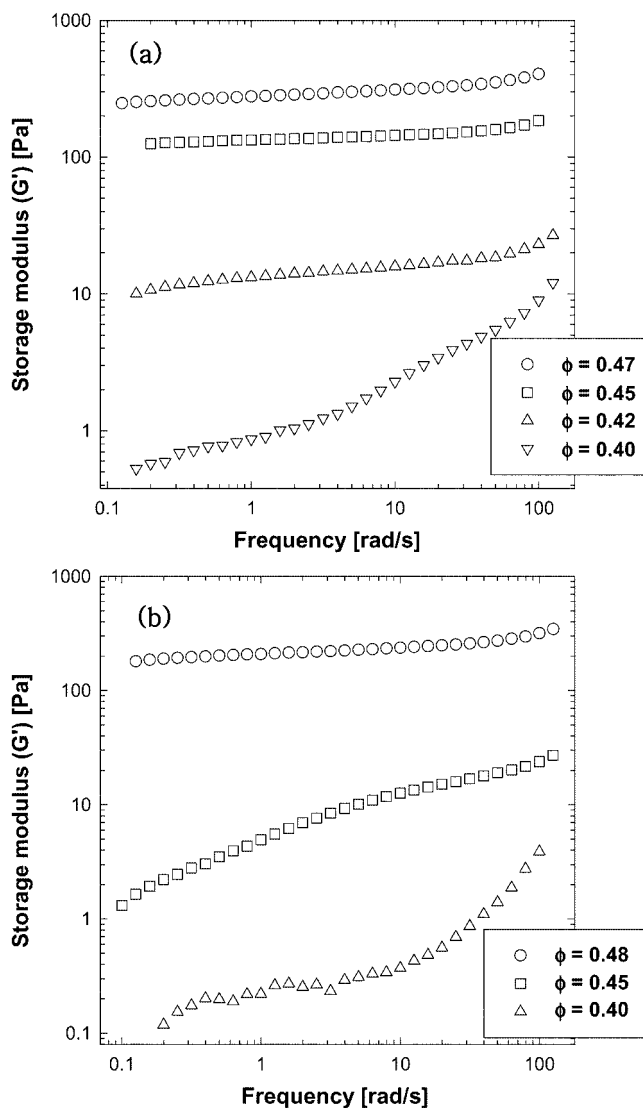


Fig. 6. Storage modulus ( $G'$ ) as a function of the frequency of charge stabilized S13S silica suspensions with (a)  $[KCl]=10^{-3}$  M, (b)  $[KCl]=10^{-2}$  M.

phase transition and finally, displayed purely elastic response (solid-like structure). These observations clearly showed that the long-range repulsive forces were diminished with the ionic strength and the microstructure transition of charged suspension was closely related to the effective size (or volume fraction). In general, as mentioned earlier, the microstructural transition of a hard sphere is a purely entropic process and determined solely by the particle volume fractions  $\phi_f=0.494$  for freezing  $\phi_m=0.545$  for melting. As shown in Fig. 7(b), HS13M suspensions underwent a transition from viscous liquid to elastic solid responses as the volume fraction increased. It is noteworthy that nearly a solid-like response was observed slightly above the freezing point ( $\phi_f=0.494$ ).

A phase diagram of charge stabilized suspensions was constructed by using oscillatory measurement. For all charge stabilized suspensions prepared in this study, the phase diagram was constructed in terms of the nominal (open symbol) or effective (filled symbol) particle volume fraction and the ionic strength as shown in Fig. 8. Indeed, the effective volume concentration was decreased due to the

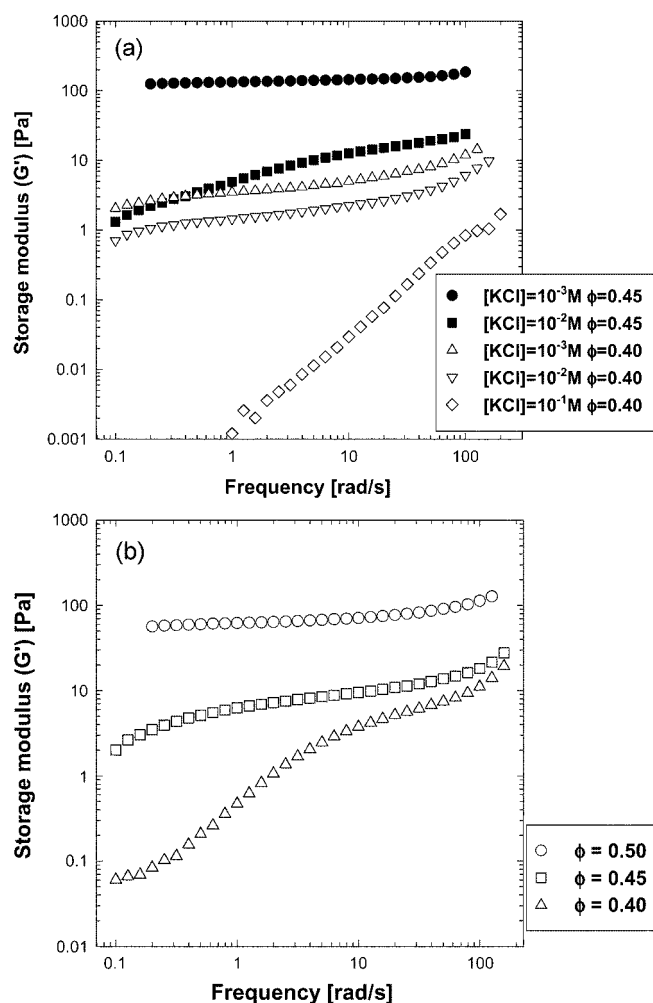


Fig. 7. Storage modulus ( $G'$ ) as a function of the frequency for (a) charge stabilized S13S silica suspensions, (b) HS13M.

double layer compressions with the salt concentration [Russel et al., 1989; Larson, 1999]. Also shown for illustrative purpose was the phase boundary of hard-sphere suspension in which phase transition occurs at  $\phi_f=0.494$  for freezing and  $\phi_m=0.545$  for melting. It can be seen clearly that the phase diagram of electrostatically stabilized suspension was well coincident with the hard-sphere phase diagram if the effective particle volume fraction was used instead of the nominal particle volume fraction. Therefore, the phase diagram clearly confirmed that charge stabilized suspensions could be also characterized by ideal 'hard-sphere' suspensions considering their effective volume determined from the surface charge potential.

## CONCLUSIONS

In the present paper, the monodisperse silica suspensions were prepared by sol-gel method and their rheological behavior and microstructural transition were investigated experimentally. In particular, the shear viscosity of charge stabilized suspension was measured and compared with the viscosity of hard sphere suspensions that have only short-range interactions. Moreover, the storage modulus ( $G'$ ) of the silica suspensions was measured to probe the transition

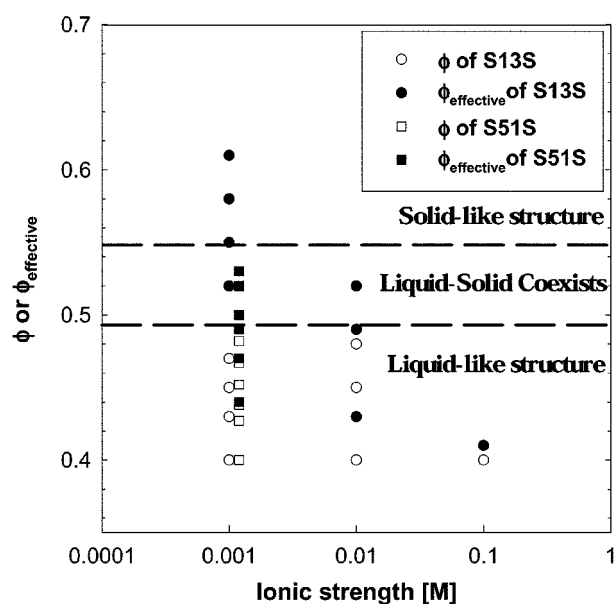


Fig. 8. Phase diagram of charge stabilized silica suspensions determined from oscillatory storage modulus measurement. Dashed lines are phase boundaries for ideal hard sphere suspensions.

from liquid-like to solid-like structure by varying the particle volume fraction, salt concentration and particle size. The conclusions from the present investigations are as follows:

1. The electrostatic repulsive forces of charge-stabilized suspensions were controlled by the salt concentration. As the salt concentration increased, the effective volume fraction of charge-stabilized suspension was decreased and the shear viscosity approached that of hard sphere suspension.
2. For a charge stabilized particle suspensions, elastic and solid-like response was enhanced as the particle volume fraction increased. Moreover, as the salt concentration increased, the transition volume fraction was also increased.
3. The viscosity at low shear rates was decreased as the particle size increased. This is due to the fact that the Brownian motion contribution diminished for the larger particle suspension.
4. A phase diagram of charge stabilized suspensions was constructed by using dynamic oscillatory measurement. The phase diagram constructed by using the effective particle volume fraction was well coincident with the hard-sphere phase diagram, and the charge stabilized suspensions could be characterized by ideal 'hard-sphere' suspension considering their effective volume determined from the surface charge potential.

## ACKNOWLEDGMENTS

This work was supported by a grant from the Ministry of Commerce, Industry and Energy. The authors also acknowledge partial support from the Brain Korea 21 project.

## REFERENCES

Barnes, H. A., Hutton, J. F. and Walters, K., "An Introduction to Rheol-

- ogy," Elsevier Science Publishers, New York, USA (1989a).
- Barnes, H. A., "Shear-Thickening (Dilatancy) in Suspension of Non-segregating Solid Particles Dispersed in Newtonian Fluids," *J. Rheol.*, **33**, 329 (1989b).
- Bogush, G. H., Tracy, M. A. and Zukoski, C. G., "Preparation of Monodisperse Silica Particles: Control of Size and Mass Fraction," *J. Non-Cryst. Solids*, **104**, 95 (1988).
- Brady, J. F., "Computer Simulation of Viscous Suspensions," *Chem. Eng. Sci.*, **56**, 2921 (2001).
- Chen, L. B., Ackerson, B. J. and Zukoski, C. F., "Rheological Consequences of Microstructural Transitions in Colloidal Crystals," *J. Rheol.*, **38**, 193 (1994).
- Chow, M. K. and Zukoski, C. F., "Nonequilibrium Behavior of Dense Suspensions of Uniform Particles: Volume Fraction and Size Dependence of Rheology and Microstructure," *J. Rheol.*, **39**, 33 (1995a).
- Chow, M. K. and Zukoski, C. F., "Gap Size and Shear History Dependencies in Shear Thickening of a Suspension Ordered at Rest," *J. Rheol.*, **39**, 15 (1995b).
- Fagan, M. E. and Zukoski, C. F., "The Rheology of Charge Stabilized Silica Suspensions," *J. Rheol.*, **41**, 373 (1997).
- Foss, D. R. and Brady, J. F., "Structure, Diffusion and Rheology of Brownian Suspensions by Stokesian Dynamics Simulation," *J. Fluid Mech.*, **407**, 167 (2000).
- Franks, G. V., Zhou, Z., Duin, N. J. and Boger, D. V., "Effect of Interparticle Forces on Shear Thickening of Oxide Suspensions," *J. Rheol.*, **44**, 759 (2000).
- Gast, A. P. and Russel, W. B., "Simple Ordering in Complex Fluids," *Physics Today*, **51**(12), 24 (1998).
- Kose, A., Ozaka, M., Takano, K., Kobayashi, Y. and Hachisu, S., "Direct Observation of Ordered Latex Suspension by Metallurgical Microscope," *J. Colloid Interface Sci.*, **44**, 330 (1973).
- Kose, A. and Hachisu, S., "Ordered Structure in Weakly Flocculated Monodisperse Latex," *J. Colloid Interface Sci.*, **55**, 487 (1976).
- Larson, R. G., "The Structure and Rheology of Complex Fluids," Oxford University Press, New York, USA (1999).
- Laun, H. M., Bung, R., Hess, S., Loose, W., Hess, O., Hahn, K., Hadicke, E., Hingmann, R., Schmidt, F. and Lindner, P., "Rheological and Small Angle Neutron Scattering Investigation of Shear-induced Particle Structures of Concentrated Polymer Dispersions Submitted to Plane Poiseuille and Couette Flow," *J. Rheol.*, **36**, 743 (1992).
- Lee, J.-D. and Yang, S.-M., "Rheo-optical Behavior and Stability of Silica Particle Suspension Coated with Silane Coupling Agents," *J. Colloid Interface Sci.*, **205**, 397 (1998).
- Lee, J.-D., So, J.-H. and Yang, S.-M., "Rheological Behavior and Stability of Concentrated Silica Suspensions," *J. Rheol.*, **43**, 1117 (1999).
- Lewis, J. A., "Colloidal Processing of Ceramics," *J. Am. Ceram. Soc.*, **83**, 2341 (2000).
- Oh, M.-H., So, J.-H., Lee, J.-D. and Yang, S.-M., "Preparation of Silica Dispersion and its Phase Stability in the Presence of Salts," *Korean J. Chem. Eng.*, **16**, 532 (1999).
- Perez, M. Q., Fernandez, J. C. and Alvarez, R. H., "Interaction Potentials, Structural Ordering and Effective Charges in Dispersions of Charged Colloidal Particles," *Adv. Colloid Interface Sci.*, **95**, 295 (2002).
- Philipse, A. P. and Vrij, A., "Preparation and Properties of Nonaqueous Model Dispersions of Chemically Modified, Charged Silica Spheres," *J. Colloid Interface Sci.*, **128**, 121 (1989).
- Quemada, D. and Berli, C., "Energy of Interaction in Colloids and its Implications in Rheological Modeling," *Adv. Colloid Interface Sci.*, **98**, 51 (2002).
- Russel, W. B., Saville, D. A. and Schowalter, W. R., "Colloidal Dispersion," Cambridge University Press, New York, USA (1989).
- So, J.-H., Bae, S., Yang, S.-M. and Kim, D., "Preparations of Silica Slurry for Wafer Polishing Via Controlled Growth of Commercial Silica Seeds," *Korean J. Chem. Eng.*, **18**, 547 (2001a).
- So, J.-H., Oh, M.-H., Lee, J.-D. and Yang, S.-M., "Effects of Polyvinyl Alcohol on the Rheological Behavior and Phase Stability of Aqueous Silica Suspensions," *J. Chem. Eng. Japan*, **34**, 262 (2001b).
- So, J.-H., Yang, S.-M. and Hyun, J. C., "Microstructure Evolution and Rheological Behavior of Hard Sphere Suspensions," *Chem. Eng. Sci.*, **56**, 2967 (2001c).
- So, J.-H., Yang, S.-M., Kim, C. and Hyun, J. C., "Microstructure and Rheological Behavior of Electrosterically Stabilized Silica Particle Suspensions," *Colloids and Surfaces A*, **190**, 89 (2001d).
- Stavov, V., Zhdanov, V., Meireles, M. and Molle, C., "Viscosity of Concentrated Suspensions: Influence of Cluster Formation," *Adv. Colloid Interface Sci.*, **96**, 279 (2002).
- Stöber, W., Fink, A. and Bohn, E., "Controlled Growth of Monodisperse Silica Spheres in the Micron Size Range," *J. Colloid Interface Sci.*, **26**, 62 (1968).
- Tadros, Th. F., "Correlation of Viscoelastic Properties of Stable and Flocculated Suspensions with their Interparticle Interactions," *Adv. Colloid Interface Sci.*, **68**, 97 (1996).